

# UC Irvine

## UC Irvine Previously Published Works

### Title

Pressure-induced superconductivity in quasi-2D CeRhIn5

### Permalink

<https://escholarship.org/uc/item/8zv0d3gw>

### Journal

Physical review letters, 84(21)

### ISSN

0031-9007

### Authors

Hegger, H  
Petrovic, C  
Moshopoulou, EG  
[et al.](#)

### Publication Date

2000-05-01

### DOI

10.1103/physrevlett.84.4986

### License

<https://creativecommons.org/licenses/by/4.0/> 4.0

Peer reviewed

## Pressure-Induced Superconductivity in Quasi-2D CeRhIn<sub>5</sub>

H. Hegger,\* C. Petrovic,† E. G. Moshopoulou,‡ M. F. Hundley, J. L. Sarrao, Z. Fisk,† and J. D. Thompson

*Los Alamos National Laboratory, Los Alamos, New Mexico 87545*

(Received 22 November 1999)

CeRhIn<sub>5</sub> is a new heavy-electron material that crystallizes in a quasi-2D structure that can be viewed as alternating layers of CeIn<sub>3</sub> and RhIn<sub>2</sub> stacked sequentially along the tetragonal *c* axis. Application of hydrostatic pressure induces a first-order-like transition from an unconventional antiferromagnetic state to a superconducting state with  $T_c = 2.1$  K.

PACS numbers: 74.70.Tx, 74.62.Fj, 75.30.Mb, 75.40.-s

The relationship between magnetism and superconductivity is a recurring theme of research on heavy-fermion materials. In these materials, the evolution of ground states as functions of pressure or chemical environment frequently is discussed in terms of an intuitively appealing, but qualitative, model first proposed by Doniach. This model [1] considers a one-dimensional chain of Kondo impurity atoms that experience the effect of competing long-range Ruderman-Kittel-Kasuya-Yosida (RKKY) and short-range Kondo interactions, both of which depend on a coupling constant proportional to the magnetic exchange  $|J|$ . Because of their different functional dependencies on  $|J|$ , quadratic (RKKY) and exponential (Kondo), RKKY interactions dominate for small values of  $|J|$ , the spin system orders magnetically, and the Néel temperature  $T_N$  increases initially with the exchange. For modest values of  $|J|$ , the magnetic singlet state favored by the Kondo effect competes with long-range order, producing a maximum in  $T_N$  versus  $|J|$ , and at sufficiently large  $|J|$  drives the magnetic state toward a zero-temperature transition. Cerium is a well-known Kondo impurity ion that, when periodically placed in an appropriate crystal lattice, orders magnetically out of a strongly correlated electron state and is well suited for comparison to the Doniach model. There are several examples [2] where pressure has been used to tune the exchange in Ce-based compounds, and the observed pressure dependence of magnetic order is qualitatively that expected from this model provided  $\partial|J|/\partial P > 0$ . Interestingly, in several of these materials, heavy-fermion superconductivity appears as the zero-temperature magnetic-nonmagnetic boundary is approached by applied pressure [3–6]. These observations support the widely held view that heavy-fermion superconductivity is mediated by spin fluctuations that are present near this boundary [7]. Experiments also show [8] that in many of these cases superconductivity develops out of an unconventional normal state in which the electrical resistivity increases quasilinearly with temperature, in contrast to the  $T^2$  dependence expected of a Landau Fermi liquid. Such non-Fermi-liquid behavior is expected [9] near a zero-temperature phase transition, where quantum-critical fluctuations dominate temperature dependencies of thermodynamic and transport properties.

Of the several Ce-based compounds whose ground states evolve as described above, all but one crystallize in the ThCr<sub>2</sub>Si<sub>2</sub> body-centered tetragonal structure; cubic CeIn<sub>3</sub>, which forms in the Cu<sub>3</sub>Au structure, is the notable exception and an archetypal example. At atmospheric pressure it orders antiferromagnetically at  $T_N \approx 10$  K in a  $\Gamma_7$  crystal-field doublet ground state, with reduced ordered moments of about  $0.5\mu_B$  that are expected as the magnetic-nonmagnetic boundary is approached. Applying pressure [5] to CeIn<sub>3</sub> monotonically reduces  $T_N$  toward zero temperature at a critical pressure  $P_c \approx 25$  kbar where superconductivity sets in at temperatures  $T_c \leq 0.25$  K, and for  $T \geq T_c$ , the resistivity follows a power law  $\rho - \rho_0 \propto T^n$ , where  $n \leq 1.5$ . In the absence of contradictory observations, the substantial body of data available for these materials has provided general validation of the qualitative interpretation that follows from Doniach's model. In the following, we present results of ambient and high-pressure studies on single crystals of CeRhIn<sub>5</sub> whose response to pressure suggests that possibilities are richer than this qualitative picture envisions.

Crystals of CeRhIn<sub>5</sub> with dimensions up to 1 cm<sup>3</sup> were grown from an In flux. X-ray diffraction showed that the material was single phase and formed in the primitive tetragonal HoCoGa<sub>5</sub> structure type, with lattice parameters  $a_0 = 4.652$  Å and  $c_0 = 7.542$  Å. In this structure, CeRhIn<sub>5</sub> can be viewed as alternating layers of CeIn<sub>3</sub> and RhIn<sub>2</sub> stacked sequentially along the *c* axis [10]. There is a single Ce site with  $4/mmm$  symmetry. The  $a_0$  parameter corresponds to that of CeIn<sub>3</sub> units in this structure and is smaller than  $a_0$  of bulk CeIn<sub>3</sub>. Taking the bulk modulus  $B = 650$  kbar [11] for CeIn<sub>3</sub>, the difference in lattice parameters implies that the CeIn<sub>3</sub> units in CeRhIn<sub>5</sub> experience a chemical pressure of approximately 14 kbar relative to three-dimensional (3D) CeIn<sub>3</sub> at atmospheric pressure.

Figure 1 summarizes ambient-pressure thermodynamic and transport properties of CeRhIn<sub>5</sub>. The total specific heat divided by temperature [Fig. 1(a)] is a minimum near 9 K, where its value is approximately 400 mJ/mole K<sup>2</sup>, before reaching a maximum at 3.8 K that signals the onset of magnetic order. The inset of Fig. 1(a) plots the entropy obtained by integrating the magnetic specific

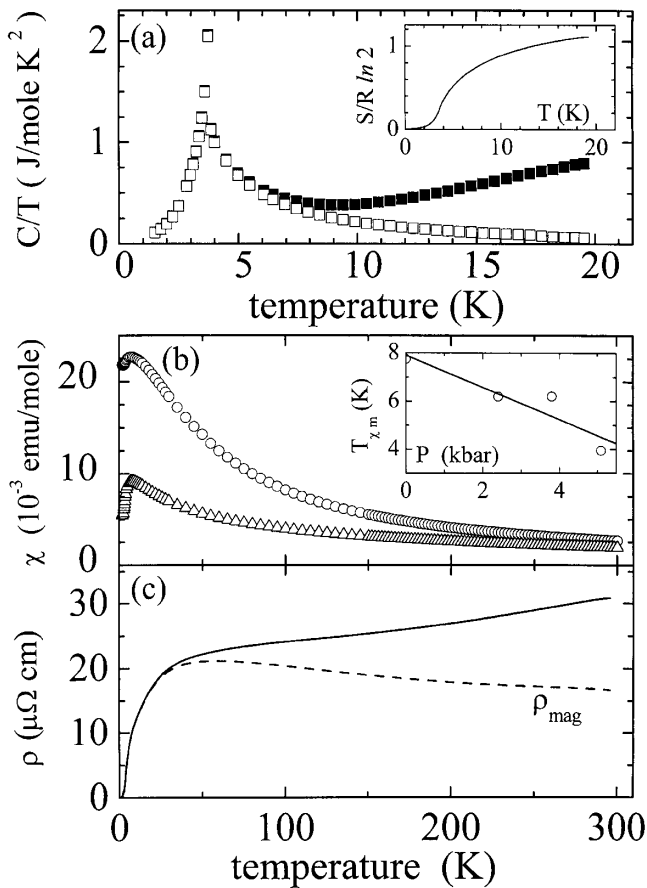


FIG. 1. (a) Specific heat divided by temperature versus temperature for  $\text{CeRhIn}_5$ . Solid symbols are the total specific heat; open symbols are the magnetic contribution to  $C/T$  estimated by subtracting the specific heat of  $\text{LaRhIn}_5$ , which has a Sommerfeld coefficient of  $5.7 \text{ mJ/mole K}^2$  and Debye temperature of  $245 \text{ K}$ . The inset shows the magnetic entropy as a function of temperature. (b) Static magnetic susceptibility  $\chi$  measured in an applied field of  $1 \text{ kOe}$  for the field along the  $c$  axis (circles) and  $a$  axis (triangles) of  $\text{CeRhIn}_5$ . The inset gives the pressure dependence of the temperature  $T_{\chi m}$  at which  $\chi$  is a maximum. The solid line is a linear fit to the data. (c) Temperature dependence of the electrical resistivity  $\rho(T)$  for  $\text{CeRhIn}_5$  (solid curve). At  $300 \text{ K}$ , the  $c$ -axis resistivity is approximately twice as large as that in the basal plane. The dashed curve is the magnetic contribution estimated by subtracting the resistivity of  $\text{LaRhIn}_5$ .

heat as a function of temperature. Only 30% of  $R \ln 2$  entropy is released below  $T_N$ , suggesting a substantial Kondo-compensated ordered moment, consistent with nuclear quadrupole resonance measurements [12] that find an ordered moment of  $(0.1-0.2)\mu_B$ . The remaining 70%  $R \ln 2$  entropy is recovered on warming to  $18-20 \text{ K}$  and is reflected in the long high-temperature tail in the magnetic contribution to  $C/T$ . From  $C/T$  data, it is difficult to define precisely the electronic specific heat above  $T_N$ , but a simple entropy-balance construction [ $S(T_N - \varepsilon) = S(T_N + \varepsilon)$ ] gives a Sommerfeld coefficient  $\gamma \geq 420 \text{ mJ/mole K}^2$ . The magnetic susceptibility  $\chi$  [Fig. 1(b)] has no detectable in-plane anisotropy and an easy axis of magnetization along the  $c$  direction.

Paramagnetic Curie-Weiss temperatures, obtained from linear fits of the inverse susceptibility for  $T > 100 \text{ K}$ , are  $-79 \text{ K}$  in the  $a$ - $b$  plane and  $+16 \text{ K}$  for the field along the  $c$  axis. A polycrystalline average of these data gives a high-temperature effective moment  $\mu_{\text{eff}} = 2.38\mu_B$ , reduced somewhat from the Hund's rule value of  $2.54\mu_B$  for  $\text{Ce}^{+3}$  by crystal-field splitting of the  $J = 5/2$  manifold, and paramagnetic Weiss temperature of  $-31 \text{ K}$ . The susceptibility exhibits a weak maximum near  $T_{\chi m} = 7.5 \text{ K}$ , independent of field direction, before dropping more steeply at  $T_N$ . Ce-based compounds, in which  $J = 5/2$ , commonly exhibit a low-temperature maximum in  $\chi$  that is expected from the theory [13] of orbitally degenerate Kondo impurities. However, specific heat measurements as well as the crystal symmetry suggest that the ground state of  $\text{CeRhIn}_5$  is doubly degenerate, in which case the Kondo effect produces the maximum susceptibility at  $T = 0$ . The electrical resistivity  $\rho$  of  $\text{CeRhIn}_5$  [Fig. 1(c)] is similar in magnitude and temperature dependence to that of bulk  $\text{CeIn}_3$ [5] and is typical of nearly defect-free cerium heavy-fermion materials: weakly temperature dependent above  $100 \text{ K}$  and falling rapidly at lower temperatures to a value of approximately  $0.4 \mu\Omega \text{ cm}$  at  $0.4 \text{ K}$ . Traditionally, this behavior is interpreted [14] as indicating a crossover from incoherent Kondo scattering at high temperatures to the formation of heavy-electron Bloch states at low temperatures. At  $3.8 \text{ K}$ , there is a weak anomaly in  $\rho(T)$  that coincides with  $T_N$  found in  $C/T$  and  $\chi$ . Together, the data in Fig. 1 establish  $\text{CeRhIn}_5$  as a new heavy-fermion compound in which an antiferromagnetic instability develops in a crystal-field doublet ground state. The small ordered moment below  $T_N$  implies the presence of relatively strong Kondo spin compensation, and, consequently, would place  $\text{CeRhIn}_5$  close to the magnetic-nonmagnetic boundary in the Doniach model.

From this perspective, applying pressure to  $\text{CeRhIn}_5$  should drive  $T_N$  toward  $T = 0$  and perhaps induce superconductivity. Figure 2 shows the resistivity measured at various applied pressures generated in a clamp-type cell [15] with Fluorinert-75 as the pressure medium. The most prominent feature of these data is the evolution of a well-defined maximum in the resistivity at a temperature  $T_{\text{max}}$ , which, as shown in the inset, initially moves to lower temperatures with increasing pressure, reaches a minimum near  $12-13 \text{ kbar}$ , and then increases at the highest pressures. This negative  $\partial T_{\text{max}}/\partial P$  is highly unusual, whereas the positive  $\partial T_{\text{max}}/\partial P \approx 1 \text{ K/kbar}$  above  $15 \text{ kbar}$  is typical of Ce-based heavy-fermion materials [2]. Pressure studies of both Ce impurities in nonmagnetic hosts [16] and of Ce-based heavy-fermion compounds [2] point to  $\partial|J|/\partial P > 0$ . Because the Kondo temperature  $T_K \propto \exp(-1/|J|)$ ,  $\partial T_K/\partial P > 0$  and  $T_{\text{max}}$  should increase with pressure. The results of Fig. 2 suggest, then, either that  $\partial|J|/\partial P < 0$  or that another mechanism is competing with the Kondo effect to produce the initial decrease of  $T_{\text{max}}$  with pressure.

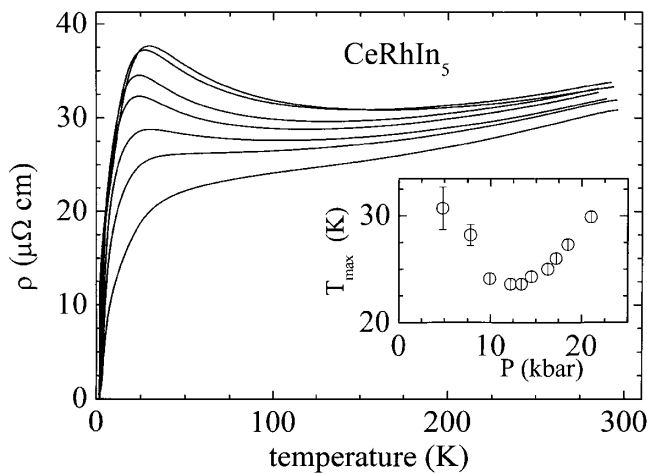


FIG. 2. Temperature dependence of the electrical resistivity of CeRhIn<sub>5</sub> at representative applied pressures. Data shown correspond to pressures of 0.001, 4.8, 7.9, 12.2, 14.5, 18.5, and 21.0 kbar and are associated, respectively, with curves of increasing resistivity at 50 K. The inset is a plot of the pressure dependence of the temperature  $T_{\max}$  where the resistivity is a maximum.

In this regard, measurements of  $\chi(T, P)$  in a SQUID magnetometer [17] to 5 kbar show [inset of Fig. 1(b)] that the temperature  $T_{\chi m}$  at which  $\chi(T)$  is a maximum decreases approximately linearly with increasing pressure and extrapolates to  $T = 0$  at  $13 \pm 4$  kbar, a value near the pressure at which  $T_{\max}(P)$  is a minimum.

The low-temperature response of the resistivity to pressure, plotted in Fig. 3, is remarkable. There is a large, reversible increase in the low-temperature resistivity; at 2.5 K,  $\rho(T, P)$  increases from less than  $1 \mu\Omega \text{ cm}$  at  $P = 1$  bar to approximately  $12 \mu\Omega \text{ cm}$  at  $P = 21$  kbar. Accompanying this increase in the magnitude of  $\rho(T, P)$

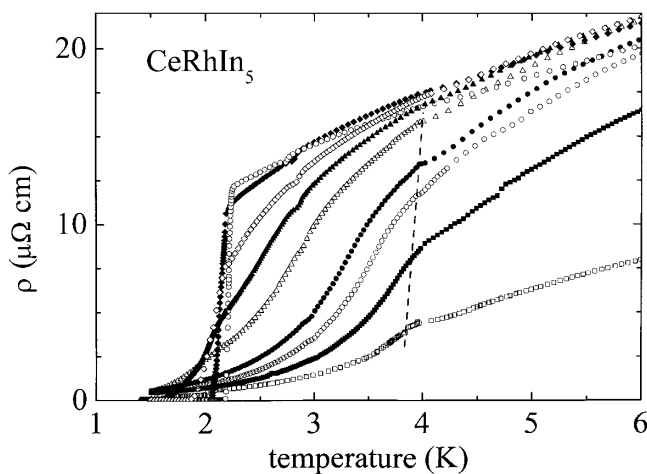


FIG. 3. Low-temperature response of CeRhIn<sub>5</sub> to applied pressures. With increasing resistivity at 2.3 K, the curves correspond to applied pressures of 0.001, 7.9, 9.9, 12.2, 14.5, 16.3, 17.2, 18.5, and 21.0 kbar. The diagonal dashed line is a guide to the eye.

is a systematic change in its temperature dependence. The Néel temperature increases weakly with pressure for  $P \leq 14.5$  kbar, above which there is no resistive signature for  $T_N$ . At 16.3 kbar and higher, there is a transition beginning near 2 K to a zero-resistance state; the transition width is initially broad and sharpens to less than 0.05 K at 21 kbar where the onset of superconductivity is at 2.17 K. Experiments to 17 kbar on a second single crystal, grown independently, reproduce the appearance of superconductivity; simultaneous measurements of the ac susceptibility of this second crystal and a piece of Sn with the same geometry show nearly identical diamagnetic responses at their respective superconducting transition temperatures. By this measure, the pressure-induced superconductivity in CeRhIn<sub>5</sub> is a bulk effect. Upper critical field measurements in fields to 10 T on the first crystal give  $-\partial H_{c2}/\partial T|_{T_c} \geq 14$  T/K at  $P = 21$  kbar.

Preliminary specific heat measurements [18] at 20.8 kbar confirm bulk heavy-fermion superconductivity but also show a relatively large anomaly at 2.75 K that clearly is not due to superconductivity of free In. Whatever the origin of this anomaly, it also is reflected in  $\rho(T)$  at 21 kbar and possibly at pressures as low as 9.9 kbar, where there is a very small change in slope near 3 K.

The  $T$ - $P$  phase diagram constructed from these data is plotted in Fig. 4. The abrupt loss of a signature for  $T_N$ , the sudden appearance of superconductivity, and the rapid sharpening of the superconducting transition width suggest a first-order-like transition at a critical pressure  $P_c$  between 14.5 and 16.3 kbar that is independent of the anomaly, labeled  $T_?$ , found in resistivity and specific heat data above 9 kbar. This phase diagram is unlike any previously reported for Ce heavy-fermion compounds [3–6] and is apparently contrary to that expected from the Doniach model.

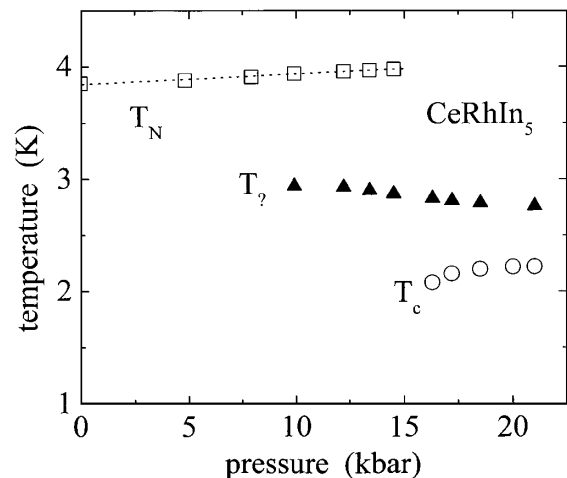


FIG. 4. Temperature-pressure phase diagram for CeRhIn<sub>5</sub> constructed from data shown in Fig. 3. Squares and circles give the pressure dependence of the Néel and onset superconducting transition temperatures, respectively. Triangles correspond to resistance features of unknown origin; see text. The dashed line has a slope of 9 mK/kbar.

The first-order-like transition is approximately coincident with the change in sign of the pressure dependence of  $T_{\max}$  and the pressure at which  $T_{\chi m}$  extrapolates to  $T = 0$ .

A qualitative interpretation of the ambient- and high-pressure properties of CeRhIn<sub>5</sub> is suggested by its quasi-2D crystal structure. The smaller  $a_0$  of CeRhIn<sub>5</sub> compared to that of bulk CeIn<sub>3</sub> implies that the CeIn<sub>3</sub> building blocks are under roughly 14 kbar chemical pressure. At 14 kbar, the Néel temperature of 3D CeIn<sub>3</sub> is 8 K [5]. It, therefore, is reasonable to associate the maximum at 7.5 K in the susceptibility of CeRhIn<sub>5</sub> with the development of 2D spin correlations in its CeIn<sub>3</sub> layers [19]. This association leads to the following implications. (1)  $T_{\chi m}$  should decrease to  $T = 0$  at a pressure of 11 kbar, which is the applied pressure required, in addition to the 14 kbar chemical pressure, to compress the CeIn<sub>3</sub> layers to an equivalent of 25 kbar (where  $T_N$  of 3D CeIn<sub>3</sub> goes to zero). This value of 11 kbar agrees with our experimental estimate of  $13 \pm 4$  kbar. (2) It is not a coincidence that  $T_{\max}$  is a minimum near the pressure where  $T_{\chi m}$  extrapolates to  $T = 0$ . As  $T_{\chi m}$  moves toward  $T = 0$ , 2D antiferromagnetic fluctuations are enhanced at low temperatures, leading to an increase in the low-temperature resistivity and the development of a maximum in  $\rho(T, P)$  that initially follows  $T_{\chi m}(P)$ . There should be a crossover from antiferromagnetic- to quantum-fluctuation dominated scattering as  $T_{\chi m} \rightarrow 0$ . (3) Néel order arises from a weak, but strongly pressure dependent, interlayer exchange  $|J|_{\perp}$ . The competition between increasing  $|J|_{\perp}$  and decreasing  $\langle \mathbf{S} \cdot \mathbf{s} \rangle$  results in a critical point at  $14.9 < P_c < 16.3$  kbar. From the preceding discussion, we would expect  $P_c$  to be somewhat lower. At present, we do not know if this difference of a few kilobars is significant or simply is within uncertainty in estimating where  $T_{\chi m} \rightarrow 0$ .

In summary, CeRhIn<sub>5</sub> is a new heavy-fermion antiferromagnet that becomes a bulk heavy-fermion superconductor at pressures above 16.3 kbar, with an initial transition temperature nearly 10 times higher than the maximum  $T_c$  of bulk CeIn<sub>3</sub> [20]. The evolution from antiferromagnetic to superconducting states is markedly different from all previous examples. CeRhIn<sub>5</sub> emphasizes the need to consider dimensionality effects in a more realistic generalization of the widely accepted views that follow from Doniach's Kondo-necklace model.

\*Present address: Bayer AG, IM-EMS-CAE1, Leverkusen, Germany.

†Permanent address: NHMFL, Florida State University, Tallahassee, FL.

‡Present address: Brookhaven National Laboratory, Physics Department, Upton, NY.

- [1] S. Doniach, in *Valence Instabilities and Related Narrow Band Phenomena*, edited by R.D. Parks (Plenum, New York, 1977), p. 169.
- [2] See, for example, J.D. Thompson and J.M. Lawrence, in *Handbook on the Physics and Chemistry of Rare Earths, Lanthanides/Actinides: Physics II*, edited by K. A. Gschneidner, L. Eyring, G.H. Lander, and G.R. Choppin (Elsevier, Amsterdam, 1994), Vol. 19, p. 383.
- [3] D. Jaccard *et al.*, *Physica* (Amsterdam) **259–261B**, 1 (1999).
- [4] S.R. Julian *et al.*, *J. Magn. Magn. Mater.* **177–181**, 265 (1998).
- [5] I.R. Walker *et al.*, *Physica* (Amsterdam) **282–287C**, 303 (1997).
- [6] R. Movshovich *et al.*, *Phys. Rev. B* **53**, 8241 (1996).
- [7] N.D. Mathur *et al.*, *Nature* (London) **394**, 39 (1998).
- [8] See, for example, *Proceedings of the Santa Barbara Workshop on Non-Fermi Liquid Phenomena* [*J. Phys. Condens. Matter* **8** (1996)].
- [9] A. Rosch, *Phys. Rev. Lett.* **82**, 4280 (1999).
- [10] E. Moshopoulou *et al.*, *Bull. Am. Phys. Soc.* **44**, 1378 (1999); Yu.N. Grin', P. Yarmolyuk, and E.I. Gladyshevskii, *Sov. Phys. Crystallogr.* **24**, 137 (1979).
- [11] G. Oomi, T. Kagayama, and J. Sakurai, *J. Mater. Process. Technol.* **85**, 220 (1999).
- [12] N. Curro *et al.* (unpublished).
- [13] V.T. Rajan, *Phys. Rev. Lett.* **51**, 308 (1983).
- [14] See, for example, Z. Fisk *et al.*, *Science* **239**, 33 (1988).
- [15] J.D. Thompson, *Rev. Sci. Instrum.* **55**, 231 (1984).
- [16] J.S. Schilling, *Adv. Phys.* **28**, 657 (1979).
- [17] Cell design based on principles in J. Diederichs *et al.*, *J. Phys. Chem. Solids* **58**, 123 (1997).
- [18] R.A. Fisher *et al.* (unpublished).
- [19] The 2D-Heisenberg model for a spin-1/2 system predicts [see, for example, L.J. deJongh and A.R. Miedema, *Adv. Phys.* **23**, 1 (1974)] a maximum in  $\chi$  at a temperature  $T_{\chi m} \approx 0.93|J|$ , which for  $T_{\chi m} = 7.5$  K gives  $|J| = 8$  K. This model also predicts that  $\chi(T_{\chi m}) \approx 0.0938Ng^2\mu_B^2/|J|$ , which, for  $g = 2$  and  $|J| = 8$  K, gives  $\chi(T_{\chi m}) \approx 1.4 \times 10^{-2}$  emu/mole, a value close to that reported in Fig. 1(b). Any deviation from ideal two-dimensionality produces long-range order at  $T_N \approx S(S+1)|J|/2 = 3.0$  K, which compares favorably to the observed Néel temperature. The relation  $T_{\chi m} \propto |J|$  implies that  $T_{\chi m}$  should increase with applied pressure, contrary to our observations. Finally, this model also predicts a maximum in specific heat near  $T_{\chi m}$  of magnitude  $0.4R$ , and, thus, a value of  $C/T_{\chi m} \approx 0.44$  J/mole K<sup>2</sup> for CeRhIn<sub>5</sub>. A peak in  $C(T)$  is not observed, although a remnant of this peak may be reflected in the long tail above  $T_N$  in the magnetic contribution to  $C/T$ . The 2D-Heisenberg model does not include Kondo effects, which might account for some of these discrepancies.
- [20] Under otherwise similar conditions, higher  $T_c$ 's are expected in quasi-2D systems relative to their 3D analogs. See P. Monthoux and G.G. Lonzarich, *Phys. Rev. B* **59**, 14 598 (1999).